# Specific and rapid effects of acoustic stimulation on the tonotopic distribution of Kv3.1b potassium channels in the adult rat

**John G. Strumbos**[1], **Daniel B. Polley**[2],[*], and **Leonard K. Kaczmarek**[1],[**]

[1] Departments of Pharmacology, Cellular and Molecular Physiology, Yale University School of Medicine, New Haven, CT. 06520., Tel: 203-785-4500, Fax: 203-785-5494

[2] Department of Hearing and Speech Sciences, Vanderbilt Bill Wilkerson Center for Otolaryngology and Communication Sciences, Vanderbilt University School of Medicine, Nashville, TN 37232

## Abstract

Recent studies have demonstrated that total cellular levels of voltage-gated potassium channel subunits can change on a time scale of minutes in acute slices and cultured neurons (Raab-Graham et al., 2006), raising the possibility that rapid changes in the abundance of channel proteins contribute to experience-dependent plasticity *in vivo*. In order to investigate this possibility, we took advantage of the medial nucleus of the trapezoid body (MNTB) sound localization circuit, which contains neurons that precisely phase-lock their action potentials to rapid temporal fluctuations in the acoustic waveform. Previous work has demonstrated that the ability of these neurons to follow high-frequency stimuli depends critically upon whether they express adequate amounts of the potassium channel subunit Kv3.1. To test the hypothesis that net amounts of Kv3.1 protein would be rapidly upregulated when animals are exposed to sounds that require high frequency firing for accurate encoding, we briefly exposed adult rats to acoustic environments that varied according to carrier frequency and amplitude modulation (AM) rate. Using an antibody directed at the cytoplasmic C-terminus of Kv3.1b (the adult splice isoform of Kv3.1), we found that total cellular levels of Kv3.1b protein – as well as the tonotopic distribution of Kv3.1b-labeled cells – was significantly altered following 30 minutes of exposure to rapidly modulated (400 Hz) sounds relative to slowly modulated (0–40 Hz, 60 Hz) sounds. These results provide direct evidence that net amounts of Kv3.1b protein can change on a time scale of minutes in response to stimulus-driven synaptic activity, permitting auditory neurons to actively adapt their complement of ion channels to changes in the acoustic environment.

### Key Terms

Fragile X Mental Retardation Protein (FMRP); Local Protein Synthesis; Medial nucleus of the trapezoid body (MNTB); Auditory brainstem; Amplitude modulation (AM); Calyx of Held

Kv3.1 is a voltage-gated potassium channel subunit that is critical for repetitive high-frequency action potential generation (Gan and Kaczmarek, 1998; Rudy and McBain, 2001). The Kv3.1 gene gives rise to two splice isoforms, Kv3.1a and Kv3.1b, which differ in the length of their C-terminal domains (Luneau et al., 1991). The longer splice variant, Kv3.1b, is regulated by protein kinase C and predominates in the mature nervous system (Kaczmarek et al., 2005). The

[**]Correspondence should be addressed to L.K.K. (leonard.kaczmarek@yale.edu).
[*]Current Address: Massachusetts Eye and Ear Infirmary, Eaton-Peabody Laboratory, Boston, MA 02114 Tel: 617-573-3745

principal neurons of the MNTB, which require this channel to encode rapid temporal modulations in auditory stimuli, have proven to be a useful model for understanding how Kv3.1b is regulated. Previous work has demonstrated that Kv3.1b protein levels and current amplitudes vary systematically across the tonotopic axis of the MNTB, with the highest levels of the channel in the medial end, corresponding to neurons that respond selectively to high-frequency sounds (Li et al., 2001; Brew and Forsythe, 2005). Chronic lack of sensory input results in the loss of this tonotopic gradient (von Hehn et al., 2004; Leao et al., 2006), however the extent to which the gradient can be modified by sensory experience is unknown. We now report that the tonotopic distribution of Kv3.1b changes on a time scale of minutes in response to specific features of the ambient sound environment.

## Experimental Procedures

### Acoustic stimulation

Twenty-seven awake adult (8–12 week-old) Sprague-Dawley rats (Charles River) were exposed to AM stimuli for a 30 minute period at 65 dB SPL in a small sound attenuating chamber. A total of six stimuli were used in the study (Fig 1). Stimuli were centered on either 4 kHz or 32-kHz carrier frequencies and one of three AM envelope conditions: a low AM rate dynamic moving ripple (0–40 Hz; DMR, Escabi and Schreiner 2002), intermediate AM rate (57–63 Hz), or high AM rate (380–420 Hz). Rats were randomly separated into six groups: Group 1a (x1 = 4 kHz, x2 = 0–40 Hz, n = 4), Group 2a (x1 = 4 kHz, x2 = 57–63 Hz, n = 4), Group 3a (x1 = 4 kHz, x2 = 380–420 Hz, n = 5), Group 1b (x1 = 32 kHz, x2 = 0–40 Hz, n = 5), Group 2b (x1 = 32 kHz, x2 = 57–63 Hz, n = 5), and Group 3b (x1 = 32 kHz, x2 = 380–420 Hz, n = 4), where x1 is the carrier frequency on which stimuli were centered, x2 is the envelope modulation range, and n is the number of rats. At the final minute of acoustic exposure, the exposure chamber was flooded with isoflurane (5% in oxygen) and rats were quickly and silently euthanized with a lethal dose of pentobarbital sodium followed by transcardial perfusion with 0.1 M phosphate-buffered saline (PBS) followed by fixative (4% paraformaldehyde in 0.1 M phosphate buffer, pH 7.4). Following post-fixation for 2 hours at 4 C, brainstem sections were cryoprotected in a solution of 30% sucrose in 0.1 M PBS and flash frozen on dry ice.

### Immunofluorescence

Frozen brains were labeled using an encrypted code such that the investigator responsible for tissue processing was fully blinded with respect to stimulus condition. Sections (35 μm) were prepared on a Leica CM 3050-S cryostat and mounted onto glass slides coated with poly-L-lysine (Sigma-Aldrich, St. Louis, MO). Sections were then permeabilized for 24–48 hours in a blocking solution containing 0.5% Triton-X 100 and 1% goat serum in PBS. Subsequently, sections were incubated with a rabbit polyclonal antibody directed at the cytoplasmic C-terminus of Kv3.1b for 60 hours at 4 C (1:500 in blocking solution; antibody production and validation described in Perney and Kaczmarek, 1997). For secondary labeling, sections were incubated with Alexa Fluor 488 goat anti-rabbit IgG (1:500 in blocking solution, Molecular Probes, Eugene, OR) for 1–2 hours at room temperature. Following immunolabeling, MNTB sections were scanned using a Zeiss LSM 510 laser scanning confocal microscope system.

### Data Analysis

Digital image quantification was carried out using ImageJ software by a blinded investigator, with sections ($n = 99$) from each of the six experimental groups randomly interspersed. Images were normalized by background subtraction (Roll Ball Radius = 50 pixels) and a threshold of 115 a.u. (on a scale of 0–255) was set for cell identification. Cells were outlined using a particle analysis algorithm (Minimum radius = 50 pixels) and images were carefully examined by a blinded investigator to exclude artifacts. In calculating mean cell optical density (O.D.), we

restricted our analysis to animals for which a minimum of three sections containing the MNTB were available (n = 27). To ensure that each animal was equally represented in our calculation, three sections were selected for each animal using the strict criterion that they contain the greatest number of identified MNTB neurons among all sections for that animal. This selection was made by an investigator who was blinded with respect to the stimulus condition of the animal. Thus, the calculation of mean optical density per cell was carried out on 84 separate sections, which yielded a total of 10,512 cells. For calculations of medial-to-lateral ratios and construction of tonotopic probability distributions, all MNTB sections were used (n=99).

## Results

*In vivo* single-unit studies have demonstrated that MNTB principal neurons synchronize their action potentials to the phase of AM sound stimuli across a wide range of modulation rates (Joris and Yin, 1998; Kadner and Berrebi, 2008; Kopp-Scheinpflug et al., 2008), making it possible to precisely control their activity patterns *in vivo* by exposing animals to AM sounds. *In vitro*, MNTB neurons from animals lacking the Kv3.1 gene can readily follow 60 Hz stimulation, but are incapable of following higher rates of stimulation such as 400 Hz (Macica et al., 2003). Thus, while Kv3.1b subunits are not expected to be required for MNTB neurons to follow AM sounds modulated at 60 Hz, high levels of Kv3.1b current should be absolutely necessary for MNTB neurons to follow AM stimulus rates such as 400 Hz. To test the hypothesis that Kv3.1b protein levels would be rapidly upregulated *in vivo* following exposure to fast – but not slow – amplitude modulation, we exposed twenty-seven adult (8–12 week old) rats to AM sound stimuli for a 30 minute period (Fig. 1). To test the corollary hypothesis that such changes would be spatially specific, we took advantage of the tonotopic organization of the MNTB by using low (4 kHz) versus high (32 kHz) pure tone carrier frequencies to target lateral versus medial regions of the MNTB, respectively. At each carrier frequency, the temporal envelope of the stimulus was amplitude modulated at either low rates ($60 \pm 5\%$ Hz; "60 Hz AM") or high rates ($400 \pm 5\%$ Hz; "400 Hz AM"). We tested the possibility that Kv3.1b expression was specifically related to rapid temporal modulation of the acoustic stimulus, and not its overall complexity, by exposing control rats to the dynamic moving ripple ("DMR"), a frequency-modulated stimulus (0 – 0.5 cycles/octave spectral contrast) with a broad range of low frequency temporal modulations (0–40 Hz) centered either on low ($4\ kHz \pm 0.5$ octaves; "4 kHz") or high ($32\ kHz \pm 0.5$ octaves; "32 kHz") carrier frequencies (Escabi and Schreiner, 2002). Animals were randomly divided into six groups corresponding to the six stimulation conditions, with 4–5 animals in each group. All tissue processing and digital image quantification was carried out by an investigator blind to the animal's stimulation condition.

To address the first hypothesis – that Kv3.1b protein levels increase *in vivo* following exposure to rapid amplitude modulation – we compared the mean intensity of Kv3.1b immunoreactivity in the MNTB after 30 minutes of sound exposure. MNTB images from each stimulus group were pooled ($n = 81$) and mean cell O.D. was computed (detailed methods in "Experimental Procedures"). At both the 4 kHz and 32 kHz frequencies, Kv3.1b immunoreactivity was significantly enhanced when sounds were amplitude modulated at 400 Hz compared to either the 60 Hz or DMR conditions (Fig. 2a,b). This was true for both 4 kHz and 32 kHz carrier frequencies (Figure 2b; one-way ANOVA with Bonferroni post-hoc test, $p < 0.001$). We also observed a significant interaction between carrier frequency and modulation rate, such that maximal Kv3.1b labeling was achieved when the high frequency tone was modulated at the fastest rate (two-way ANOVA with Bonferroni post-hoc test, $p < 0.001$).

We tested the second hypothesis – that changes in Kv3.1b levels are localized to specific regions of the MNTB – by quantifying the pattern of Kv3.1b immunoreactivity in animals exposed to 4 versus 32 kHz carrier frequencies. Each MNTB section ($n = 99$) was divided into 550 μm halves along the tonotopic axis and the number of Kv3.1b-immunoreactive cells in

each half was quantified. A tonotopic ratio (medial immunoreactivity/lateral immunoreactivity) was calculated for each section, and all sections from each stimulus group were then pooled to compute group means. As stated above, low (4 kHz) carrier frequencies target the lateral region of the MNTB while high (32 kHz) carrier frequencies target the medial region. Consistent with our hypothesis, we found that in each of the 4 kHz conditions, the medial-to-lateral ratio of Kv3.1b-immunoreactive cells was lower than the medial-to-lateral ratios observed in rats exposed to 32 kHz tones (Figure 3a; two-way ANOVA with Bonferroni post-hoc test, $p < 0.01$). The number of Kv3.1b-immunoreactive cells per section did not vary significantly between stimulus conditions ($\mu = 92$, $\sigma = 34$).

To facilitate comparisons of Kv3.1b immunoreactivity patterns throughout the entire MNTB, we determined the precise locations of all Kv3.1b-immunoreactive cells along the tonotopic axis in each section, then pooled together all available cells from each stimulus condition ($N = 9,688$). We then created a tonotopic probability distribution for each stimulus representing the relative proportion of Kv3.1b-labeled cells in 50 μm-wide bins along the tonotopic axis. For all three amplitude modulation conditions, there was a significant difference between the two carrier frequencies in the median location of identified cells (Kolmogorov–Smirnov test, DMR: $p < 0.001$; 60 Hz: $p < 0.02$; 400 Hz: $p < 4.0 \times 10^{-12}$). Whereas the tonotopic probability distribution was only weakly influenced by carrier frequency when the stimulus was modulated slowly (DMR and 60 Hz), it shifted dramatically toward the medial end when the 32 kHz stimulus was modulated at 400 Hz and toward the lateral end when the 4 kHz stimulus was modulated at 400 Hz (Figure 3b). This observation, as well as our finding that labeling intensity was significantly enhanced by both stimuli at 400 Hz, suggests that Kv3.1b levels in MNTB principal neurons are increased selectively by rapid temporal envelope modulations.

## Discussion

The amount of Kv3.1b current in an MNTB principal neuron determines its ability to follow high rates of synaptic stimulation (Macica et al., 2003; Song et al., 2005). One established mechanism by which Kv3.1b currents become enhanced to permit high frequency firing is through dephosphorylation at Ser503 (Macica et al., 2003). Whereas Kv3.1b is basally phosphorylated at Ser503 under quiet/control conditions, it undergoes dephosphorylation following seconds to minutes of auditory stimulation *in vivo* or synaptic stimulation *in vitro* (Song et al., 2005; Song and Kaczmarek, 2006). It is not clear, however, whether changes in the phosphorylation state of the protein can provide a persistent enhancement of $K^+$ currents nor whether post-translational modification alone provides neurons with an adequate dynamic range of Kv3.1 current. Our present results provide evidence that levels of Kv3.1b channel subunits, which serve to rapidly repolarize the membrane potential during trains of high-frequency firing, can become altered within 30 minutes of a change in the auditory environment. Although we are not able to determine the time course over which these newly synthesized channels are inserted into the plasma membrane *in vivo*, an increase in Kv3.1b membrane expression would serve to maintain the increase in Kv3.1b current that is triggered by dephosphorylation of pre-existing Kv3.1b channels, and allow the neurons to maintain firing action potentials at high rates. Direct measurements of changes in Kv3.1b protein in the plasma membrane will require either electron microscopic techniques or *in vitro* brain slice models of this i*n vivo* phenomenon to quantify expression by approaches such as surface biotinylation.

Previous *in vivo* studies examining the effects of afferent activity on Kv3.1 protein levels in central neurons have focused on chronic sensory deprivation. In the avian nucleus magnocellularis, Kv3.1 protein levels decline within 3 hours of cochlear ablation and return to baseline within 24 hours (Lu et al., 2004). Additionally, it has been shown that the normal tonotopic gradient in Kv3.1b levels within the MNTB is absent in both congenitally deaf mice (Leao et al., 2006) and in mice that gradually lose hearing throughout life (von Hehn et al.,

2004). In the developing visual cortex, long-term sensory deprivation by dark rearing results in an upregulation in Kv3.1b and Kv3.2 protein levels in fast-spiking cortical basket cells that can be observed within 30 days (Grabert and Wahle, 2009). To the best of our knowledge, however, the present study is the first to report rapid alterations of the gross anatomical distribution of a voltage-gated ion channel in adult animals in response to specific features of sensory stimuli. The most striking aspect of these results is the exceedingly short time course of only 30 minutes over which auditory stimulation altered Kv3.1b immunoreactivity in the MNTB, which is comparable to amount of time required to observe stimulus-induced changes in immunoreactivity for proteins encoded by immediate early genes such as c-Fos (e.g. Graybiel et al., 1990).

Activity-dependent regulation of Kv3.1b mRNA has been shown to require 6 hours *in vitro* (Liu and Kaczmarek, 1998), therefore it seems unlikely that transcriptional mechanisms can contribute to such rapid adjustment of Kv3.1b levels during brief periods of sound stimulation. Moreover, we performed all immunohistochemistry on membrane-permeabilized tissue using an antibody directed at the cytoplasmic C-terminus of the channel, which eliminates the possibility that the increase in Kv3.1b immunoreactivity resulted from activity-dependent protein trafficking (Misonou et al., 2004; Misonou and Trimmer, 2004; Kim et al., 2007). Our findings are most readily explained by a rapid increase in Kv3.1b protein synthesis and/or turnover in response to stimulus-evoked synaptic activity. This hypothesis is consistent with recent findings in hippocampal slices and cultured neurons indicating that levels of the voltage-gated potassium channel Kv1.1 in dendrites can be rapidly altered by activity-dependent regulation of local protein synthesis (Raab-Graham et al., 2006). Moreover, although Kv3.1 protein expression varies along the tonotopic axis, there appears to be no gradient of Kv3.1 mRNA in the MNTB, indicating that, as has been found for many other proteins, levels of Kv3.1b subunits do not directly reflect levels of its mRNA (Perney et al., 1992; Perney and Kaczmarek, 1997; Li et al., 2001). Intriguingly, Kv3.1 mRNA has been identified as a candidate binding partner for FMRP, a protein that regulates rapid activity-dependent translation from preexisting mRNAs (Darnell et al., 2001). Electron microscopy studies have shown that Kv3.1b is present on both pre- and post-synaptic membranes in the MNTB (Elezgarai et al., 2003), raising the possibility that FMRP could mediate local activity-dependent translation of Kv3.1b in synaptic terminals as well as in the postsynaptic somata. An increase in pre-synaptic Kv3.1b would result in action potential narrowing and a decrease in the amount of neurotransmitter released for each spike. These data suggest that rapid adjustments in intrinsic electrical excitability may compliment established contributions from ligand-gated receptor dynamics (von Gersdorff and Borst, 2002; Takahashi et al., 2003; Sarro et al., 2008) and local network plasticity (Dean et al., 2008; Polley et al., 2004) as a homeostatic mechanism to link cellular excitability to sensory experience.

## Acknowledgments

## Abbreviations

| | |
|---|---|
| *AM* | Amplitude modulation |
| *au* | Arbitrary Units |
| *DMR* | Dynamic moving ripple |
| *Hz,kHz* | Hertz, kilohertz |
| *MNTB* | Medial nucleus of the trapezoid body |

OD          Optical Density

SPL         Sound pressure level

## References

Brew HM, Forsythe ID. Systematic variation of potassium current amplitudes across the tonotopic axis of the rat medial nucleus of the trapezoid body. Hear Res 2005;206:116–132. [PubMed: 16081003]

Darnell JC, Jensen KB, Jin P, Brown V, Warren ST, Darnell RB. Fragile X mental retardation protein targets G quartet mRNAs important for neuronal function. Cell 2001;107:489–499. [PubMed: 11719189]

Dean I, Robinson BL, Harper NS, McAlpine D. Rapid neural adaptation to sound level statistics. J Neurosci 2008;28:6430–6438. [PubMed: 18562614]

Elezgarai I, Diez J, Puente N, Azkue JJ, Benitez R, Bilbao A, Knopfel T, Donate-Oliver F, Grandes P. Subcellular localization of the voltage-dependent potassium channel Kv3.1b in postnatal and adult rat medial nucleus of the trapezoid body. Neuroscience 2003;118:889–898. [PubMed: 12732235]

Escabi MA, Schreiner CE. Nonlinear spectrotemporal sound analysis by neurons in the auditory midbrain. J Neurosci 2002;22:4114–4131. [PubMed: 12019330]

Gan L, Kaczmarek LK. When, where, and how much? Expression of the Kv3.1 potassium channel in high-frequency firing neurons. J Neurobiol 1998;37:69–79. [PubMed: 9777733]

Grabert J, Wahle P. Visual experience regulates Kv3.1b and Kv3.2 expression in developing rat visual cortex. Neuroscience 2009;158:654–664. [PubMed: 18708127]

Graybiel AM, Moratalla R, Robertson HA. Amphetamine and cocaine induce drug-specific activation of the c-fos gene in striosome-matrix compartments and limbic subdivisions of the striatum. Proc Natl Acad Sci U S A 1990;87:6912–6916. [PubMed: 2118661]

Itri JN, Michel S, Vansteensel MJ, Meijer JH, Colwell CS. Fast delayed rectifier potassium current is required for circadian neural activity. Nat Neurosci 2005;8:650–656. [PubMed: 15852012]

Joris PX, Yin TC. Envelope coding in the lateral superior olive. III. Comparison with afferent pathways. J Neurophysiol 1998;79:253–269. [PubMed: 9425196]

Kaczmarek LK, Bhattacharjee A, Desai R, Gan L, Song P, von Hehn CA, Whim MD, Yang B. Regulation of the timing of MNTB neurons by short-term and long-term modulation of potassium channels. Hear Res 2005;206:133–145. [PubMed: 16081004]

Kadner A, Berrebi AS. Encoding of temporal features of auditory stimuli in the medial nucleus of the trapezoid body and superior paraolivary nucleus of the rat. Neuroscience 2008;151:868–887. [PubMed: 18155850]

Kim J, Jung SC, Clemens AM, Petralia RS, Hoffman DA. Regulation of dendritic excitability by activity-dependent trafficking of the A-type K+ channel subunit Kv4.2 in hippocampal neurons. Neuron 2007;54:933–947. [PubMed: 17582333]

Kopp-Scheinpflug C, Tolnai S, Malmierca MS, Rubsamen R. The medial nucleus of the trapezoid body: comparative physiology. Neuroscience 2008;154:160–170. [PubMed: 18436383]

Leao RN, Sun H, Svahn K, Berntson A, Youssoufian M, Paolini AG, Fyffe RE, Walmsley B. Topographic organization in the auditory brainstem of juvenile mice is disrupted in congenital deafness. J Physiol 2006;571:563–578. [PubMed: 16373385]

Li W, Kaczmarek LK, Perney TM. Localization of two high-threshold potassium channel subunits in the rat central auditory system. J Comp Neurol 2001;437:196–218. [PubMed: 11494252]

Liu SQ, Kaczmarek LK. Depolarization selectively increases the expression of the Kv3.1 potassium channel in developing inferior colliculus neurons. J Neurosci 1998;18:8758–8769. [PubMed: 9786983]

Lu Y, Monsivais P, Tempel BL, Rubel EW. Activity-dependent regulation of the potassium channel subunits Kv1.1 and Kv3.1. J Comp Neurol 2004;470:93–106. [PubMed: 14755528]

Luneau CJ, Williams JB, Marshall J, Levitan ES, Oliva C, Smith JS, Antanavage J, Folander K, Stein RB, Swanson R, et al. Alternative splicing contributes to K+ channel diversity in the mammalian central nervous system. Proc Natl Acad Sci U S A 1991;88:3932–3936. [PubMed: 2023941]

Macica CM, von Hehn CA, Wang LY, Ho CS, Yokoyama S, Joho RH, Kaczmarek LK. Modulation of the kv3.1b potassium channel isoform adjusts the fidelity of the firing pattern of auditory neurons. J Neurosci 2003;23:1133–1141. [PubMed: 12598601]

Misonou H, Mohapatra DP, Park EW, Leung V, Zhen D, Misonou K, Anderson AE, Trimmer JS. Regulation of ion channel localization and phosphorylation by neuronal activity. Nat Neurosci 2004;7:711–718. [PubMed: 15195093]

Misonou H, Trimmer JS. Determinants of voltage-gated potassium channel surface expression and localization in Mammalian neurons. Crit Rev Biochem Mol Biol 2004;39:125–145. [PubMed: 15596548]

Perney TM, Marshall J, Martin KA, Hockfield S, Kaczmarek LK. Expression of the mRNAs for the Kv3.1 potassium channel gene in the adult and developing rat brain. J Neurophysiol 1992;68:756–766. [PubMed: 1432046]

Perney TM, Kaczmarek LK. Localization of a high threshold potassium channel in the rat cochlear nucleus. J Comp Neurol 1997;386:178–202. [PubMed: 9295146]

Polley DB, Heiser MA, Blake DT, Schreiner CE, Merzenich MM. Associative learning shapes the neural code for stimulus magnitude in primary auditory cortex. Proc Natl Acad Sci U S A 2004;101:16351–16356. [PubMed: 15534214]

Raab-Graham KF, Haddick PC, Jan YN, Jan LY. Activity- and mTOR-dependent suppression of Kv1.1 channel mRNA translation in dendrites. Science 2006;314:144–148. [PubMed: 17023663]

Rudy B, McBain CJ. Kv3 channels: voltage-gated K+ channels designed for high-frequency repetitive firing. Trends Neurosci 2001;24:517–526. [PubMed: 11506885]

Sarro EC, Kotak VC, Sanes DH, Aoki C. Hearing loss alters the subcellular distribution of presynaptic GAD and postsynaptic GABAA receptors in the auditory cortex. Cereb Cortex 2008;18:2855–2867. [PubMed: 18403398]

Song P, Yang Y, Barnes-Davies M, Bhattacharjee A, Hamann M, Forsythe ID, Oliver DL, Kaczmarek LK. Acoustic environment determines phosphorylation state of the Kv3.1 potassium channel in auditory neurons. Nat Neurosci 2005;8:1335–1342. [PubMed: 16136041]

Song P, Kaczmarek LK. Modulation of Kv3.1b potassium channel phosphorylation in auditory neurons by conventional and novel protein kinase C isozymes. J Biol Chem 2006;281:15582–15591. [PubMed: 16595659]

Takahashi T, Svoboda K, Malinow R. Experience strengthening transmission by driving AMPA receptors into synapses. Science 2003;299:1585–1588. [PubMed: 12624270]

von Gersdorff H, Borst JG. Short-term plasticity at the calyx of held. Nat Rev Neurosci 2002;3:53–64. [PubMed: 11823805]

von Hehn CA, Bhattacharjee A, Kaczmarek LK. Loss of Kv3.1 tonotopicity and alterations in cAMP response element-binding protein signaling in central auditory neurons of hearing impaired mice. J Neurosci 2004;24:1936–1940. [PubMed: 14985434]
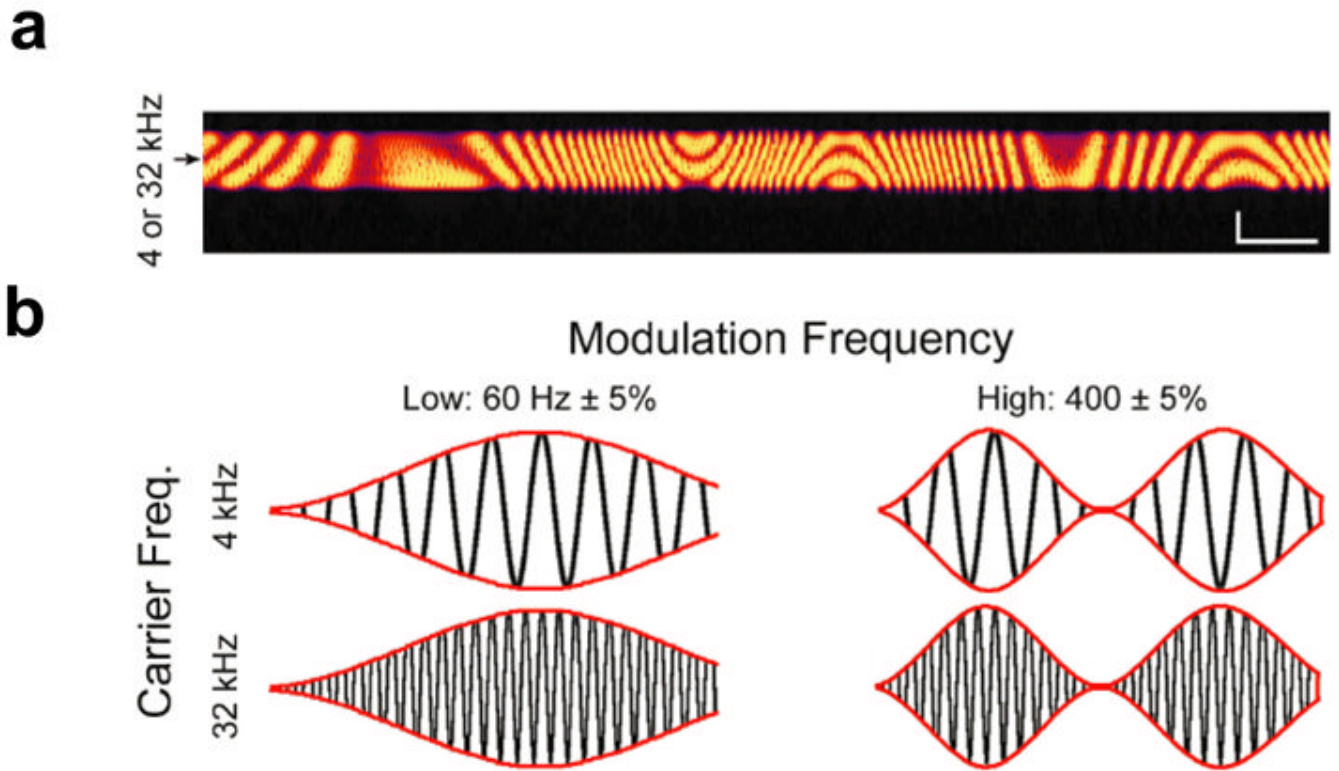
**Figure 1. Illustrations of auditory stimuli**
**(a)** Spectrogram of the complex control stimulus (dynamic moving ripple; "DMR") composed of 0.5 octave-wide sounds centered on either low (3.36–4.76 kHz; "4 kHz") or high (26.9–38.06 kHz; "32 kHz") frequencies. The DMR is smoothly and randomly modulated both in time (0–40 Hz) and frequency (spectral contrast between 0–0.5 cycles/octave). Scale bars represent 1 second and 0.25 octaves along the horizontal and vertical arms, respectively.
**(b)** AM sound stimuli were carried by either 4 kHz or 32 kHz pure tones and modulated at either low rates (60 Hz ± 5 %) or high rates (400 Hz ± 5 %).
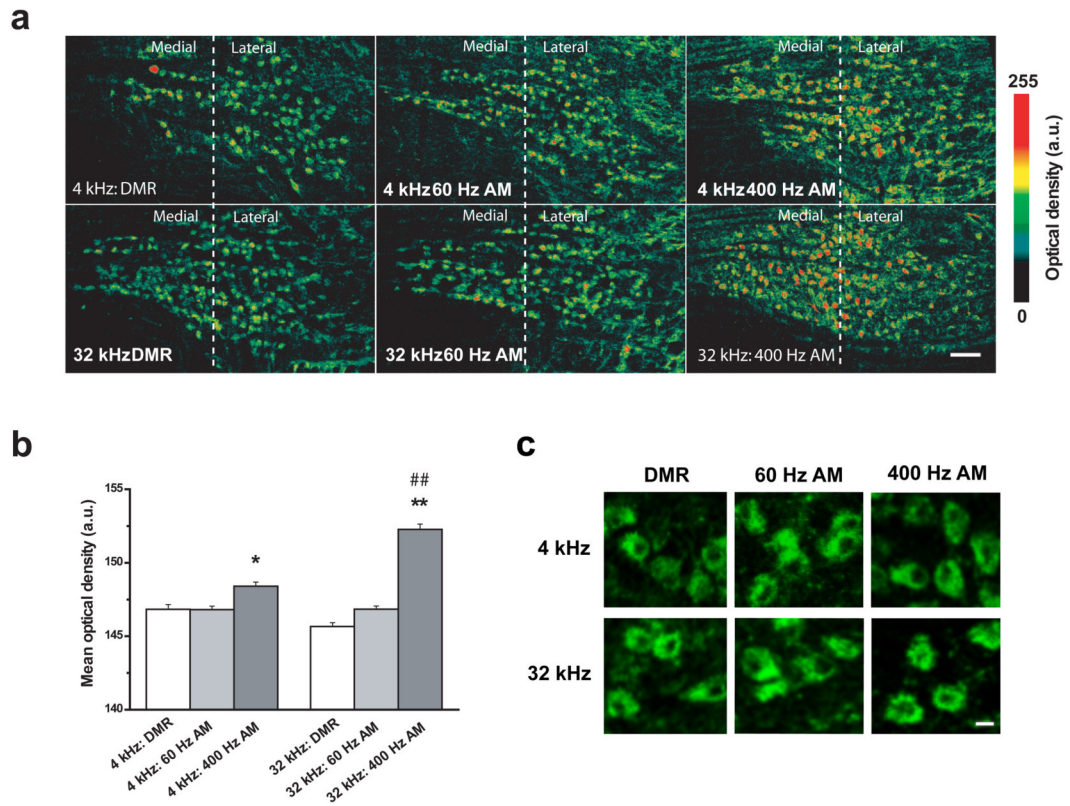
**Figure 2. Effects of sound amplitude modulation and carrier frequency on Kv3.1b levels in the MNTB**

**(a)** Pseudocolor images showing the pattern and intensity of Kv3.1b labeling in representative MNTB sections from rats belonging to each of the six stimulus groups. Scale bar: 100 μm.

**(b)** Kv3.1b labeling intensity following 30 minutes of acoustic stimulation varies according to both the carrier frequency and modulation rate of the stimulus, with the highest levels of Kv3.1b immunoreactivity observed when the high-frequency tone is modulated at the fastest rate. Data are presented as means ± S.E. The number of cells ($N$) in each stimulus condition were as follows: $N$ (4 kHz: DMR) = 1,333; $N$ (4 kHz: 60 Hz AM) = 1,763; $N$ (4 kHz: 400 Hz AM) = 1,481; $N$ (32 kHz: DMR) = 1,970; $N$ (32 kHz: 60 Hz AM) = 2,430; $N$ (32 kHz: 400 Hz AM) = 1,535. Differences between groups were statistically evaluated using both a one-way and two-way ANOVA followed by Bonferroni post-hoc analyses. * indicates $p < 0.01$ compared to other 4 kHz stimuli; ** indicates $p < 0.001$ compared to other 32 kHz stimuli; ## indicates two-way interaction of $p < 0.001$ between carrier frequency and modulation rate.

**(c)** High-magnification confocal images of Kv3.1b immunofluorescence in representative cells from each sound stimulation condition. The subcellular pattern of Kv3.1b immunofluorescence was consistent with the channel's known membrane and cytoplasmic localization (Li et al., 2001; Elezgarai et al., 2003) and did not vary across stimulation conditions. Scale bar: 0.25 μm.
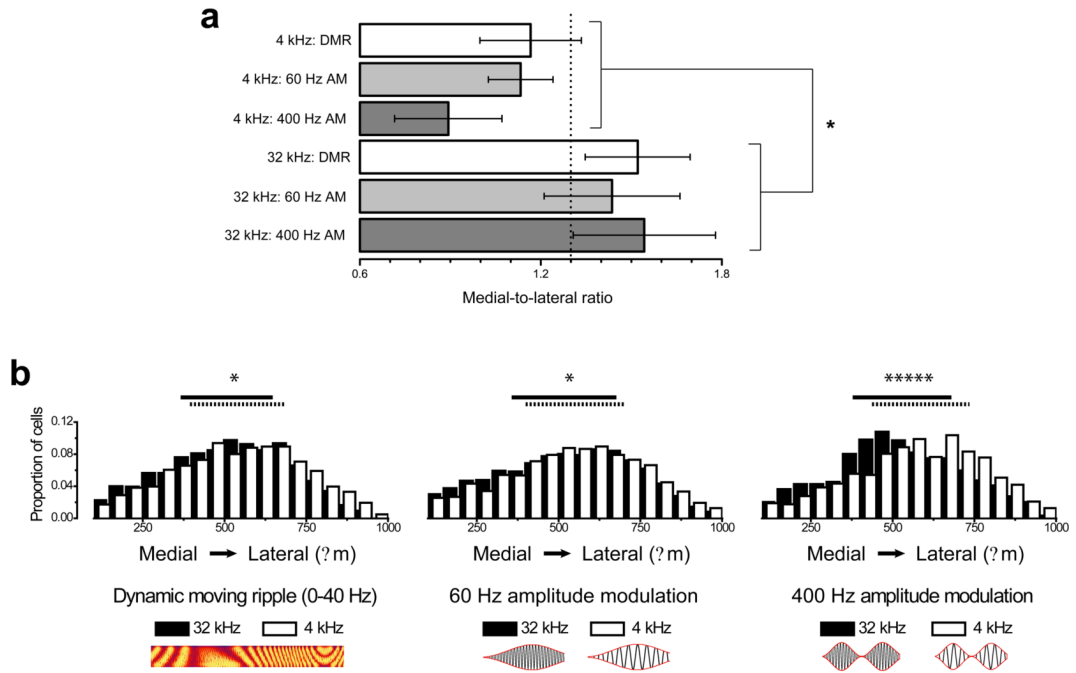
**Figure 3. Effects of carrier frequency on distribution of Kv3.1b immunoreactivity along the tonotopic axis of the MNTB**

**(a)** The medial-to-lateral ratio of Kv3.1b-labelled cells varies according to the carrier frequency of the stimulus. Data are presented as means ± S.E. * indicates p < 0.01. The dotted line represents the average medial-to-lateral ratio across all groups (1.30 ± 0.08). The number of sections (*n*) in each stimulus condition were as follows: *n* (4 kHz: DMR) = 15; *n* (4 kHz: 60 Hz AM) = 14; *n* (4 kHz: 400 Hz AM) = 15; *n* (32 kHz: DMR) = 19; *n* (32 kHz: 60 Hz AM) = 23; *n* (32 kHz: 400 Hz AM) = 13. Differences between groups were statistically evaluated using a two-way ANOVA

**(b)** Probability histograms of pooled cells in each condition demonstrate that the 400 Hz AM stimuli had a stronger effect (D = 0.15) on the distributions of Kv3.1 in the MNTB than either the 60 Hz AM (D = 0.049) or the DMR (D = 0.076) stimuli. * indicates p < 0.02, ***** indicates p < 4.0 × 10^{-12}. Lines above the probability histograms span the median 50% of cells in each distribution (solid lines represent 32 kHz stimuli, dotted lines represent 4 kHz stimuli). The number of cells (*N*) in each stimulus condition were as follows: *N* (4 kHz: DMR) = 1,384; *N* (4 kHz: 60 Hz AM) = 1,637; *N* (4 kHz: 400 Hz AM) = 1,475; *N* (32 kHz: DMR) = 1,828; *N* (32 kHz: 60 Hz AM) = 2,264; *N* (32 kHz: 400 Hz AM) = 1,118.